Regular Article

ANALYTICAL
AND BIOANALYTICAL
CHEMISTRY
RESEARCH
Published by the
Iranian Chemical Society

***Anal. Bioanal. Chem. Res.**, Vol. 11, No. 1, 77-90, January 2024.*

Study on Efficiency of HKUST-1 Metal-organic Framework and Modified HKUST-1s for Removal of Meloxicam from Aqueous Solution

Masoumeh Mohammadnejad* and Alieh Moeinipour

Department of Analytical Chemistry, Faculty of Chemistry, Alzahra University, Tehran, Iran

(Received 29 July 2023, Accepted 9 November 2023)

In the present study, HKUST-1 (Hong Kong University of Science and Technology), HKUST-1@PVA (PVA: polyvinyl alcohol), and Fe_3O_4@HKUST-1, metal-organic framework, were synthesized by hydrothermal, post-synthetic modification and pre-synthetic modification methods, respectively. These sorbents were applied to remove the meloxicam drug as the model drug from aqueous solutions. The adsorption isotherm, kinetic, and thermodynamic experiments were done and confirmed that the adsorption behaviors of HKUST-1, Fe_3O_4@HKUST-1, and HKUST-1@PVA are based on Langmuir isotherm (the values of q_{max} were obtained as 883.33, 2.50E+03 mg g^{-1} for HKUST-1@PVA and Fe_3O_4@HKUST-1, respectively) and Freundlich isotherm (the values of K_F were obtained as 3.02E+03 (n = 0.74), 7.24E+03 (n = 0.99) and 7.99E+04 (n = 1.49) for HKUST-1, Fe_3O_4@HKUST-1 and HKUST-1@PVA, respectively), with an endothermic mechanism and enthalpy-driven process. The kinetic results showed well-fitting with the pseudo-second-order kinetic model for all of them. The speed of the adsorption process, low cost, high efficiency, and high surface area are the main advantages of the proposed compounds as sorbents. The functionalization of HKUST-1 with magnetic nanoparticles decreased the adsorption time. PVA provides more functional groups on the surface of HKUST-1 and increases its adsorption efficiency. Further, an easy separation with an external magnet in 30 s is another advantage of magnetic functionalization. The aforementioned features make these adsorbents appropriate candidates for cost-effective water treatment.

Keywords: HKUST-1 Metal-organic Frameworks, HKUST-1@PVA, Fe_3O_4@HKUST-1, Meloxicam, Removal, Nonlinear Langmuir isotherm

INTRODUCTION

Metal-organic frameworks (MOFs) are considered an interesting group of crystalline porous materials containing regular porous networks which are composed of interconnected metal cations or anions clusters by coordination bonds with organic ligands as linkers. MOFs have unique structural characterizations such as a large range in pore sizes, high surface areas, specific adsorption affinities, controllable particle dimensions and morphology, uniform structured cavities and tunnels, modifiable pores, and an abundant of adjustable surface functionalities [1], which make them highly attractive sorbents for removing pollutants [2].

Using chemical groups or other components enables an easy modification of MOFs. To functionalize MOFs, pre-synthetic and post-synthesis modification methods can be applied. Particular modification is highly helpful for target pollutants' removal, and further improving the MOFs' performance via surface structure optimization [3].

Pharmaceutical compounds are expressed as the highly considerable group of environmental pollutants frequently released into wastewater. The inefficient treatment of these compounds by conventional methods resulted in their recurring detection in water resources such as sewage effluents, surface water, groundwater, and drinking water [4], affecting human health and/or ecosystems negatively.

*Corresponding author. E-mail: m.mohammadnejad@alzahra.ac.ir

Remedying water pollution by MOFs is one of the cost-effective technologies [4]. To enhance their performance, MOFs were functionalized with other materials such as magnetic material and Polyvinyl alcohol (PVA) [5]. PVA's symmetrical and regular film-forming capability, emulsification, and adhesion make it suitable for this application. In addition, PVA is a water-soluble polymer that contains a large number of polar hydroxyl groups on the molecular chain. Further, PVA is widely used due to its non-toxicity, biodegradability, and low cost for preparing cryogel material [6]. Coupling of this organic compound with MOFs results in the production of selective materials with high specific surface area, and higher removal efficiency [7].

In the present study, HKUST-1s were synthesized and applied as sorbent. HKUST-1's large surface area, high pore volume, high chemical stability, and high structural stability have made it one of the most cited MOFs, also known as MOF-199 [8,9]. HKUST-1(Hong Kong University of Science and Technology) is a coordination of Cu^{2+} ions and benzene-1,3,5-tricarboxylate (BTC) ligands [10,11]. HKUST-1 was selected as the sorbent for the removal of Meloxicam (MLX) as a non-steroidal anti-inflammatory drug (NSAIDs) from water. The widespread application of NSAIDs due to their analgesic, antipyretic, and anti-inflammatory effects on humans, livestock, and fisheries, results in their easy transportation into water systems [12]. MLX, a commonly used enol-carboxamide NSAID, has been detected in river water and effluents of wastewater treatment plants despite its poor water solubility. Alkaline wash solutions used for cleaning production lines resulted in increasing the aqueous solubility of MLX up to 17.90 mg ml^{-1} at pH = 10.7 [13-17].

In addition, HKUST-1 was functionalized with PVA (for enhancing the polarity of HKUST-1, resulting in an increased adsorption capacity), and Fe_3O_4 (to increase the speed of separation of MOF particles from water by an external magnetic field, magnetization was used [5]) by post-synthetic and pre-synthetic modification respectively, as simple and facile methods. Then, these functionalized HKUST-1s were applied to remove the non-steroidal anti-inflammatory meloxicam drug from aqueous solutions.

This is the main reason for this research. Indeed, our goal is to introduce HKUST-1 as a sorbent that can be used in water purification filters [18] (the ability to connect to all kinds of polymers with OH functional groups such as PVA), and also to be used in the industry for the direct treatment of industrial wastewater with the ability to easily separate and recover and use several times (by magnetization with the magnetic material like Fe_3O_4).

EXPERIMENTAL

Chemicals, Instruments, Synthesis of Sorbents, and Characterization

Meloxicam (MLX, (4-hydroxy-2-methyl-N-(5-methyl-2-thiazolyl)-2H-1,2-benzothiazine-3-carboxamide-1)), benzene-1,3,5-tricarboxylic acid (H_3BTC), $Cu(NO_3)_2.3H_2O$, Ferric trichloride ($FeCl_3.6H_2O$), Ferrous sulfate ($FeSO_4.7H_2O$), Ethanol, Dimethyl sulfoxide (DMSO), Polyvinyl alcohol (PVA), and Ammonia solution ($NH_3.H_2O$, 25%) were provided by Merck (Rahway, New Jersey, United States) and Sigma Aldrich company(St. Louis, Missouri, United States). All solvents and reactants were at analytical grade. All solutions were prepared using deionized water. Heidolph heater stirrer, model F60 FALC, was employed for stirring the solutions. A glass pH electrode (Metrohm 713 pH-meter) was used for pH measurement. The morphology of samples was studied by field emission scanning electron microscopy (FE-SEM), KYKY-EM 3200 with gold coating. Fourier transform infrared spectroscopy (FT-IR) spectra were obtained in Equinox 55 BRUKER, model FT-IR spectrometer and vibrating sample magnetometer (VSM) was done by VSM Meghnatis Daghigh Kavir Co. The absorbance was measured by a double-beam UV-Vis spectrophotometer using a 1 cm quartz cell (Perkin-Elmer, Lambda 35, USA). An ultrasonic bath (Transsonic TI-H-5, Elma, Singen, Germany) was used to increase the speed of the desorption step *via* ultrasonic irradiation.

Synthesis of Sorbents

Hydrothermal synthesis of HKUST-1. HKUST-1 crystals were prepared by the following hydrothermal reaction: 1.087 g (4.5 mmol) of $Cu(NO_3)_2.3H_2O$ was dissolved in 15 ml of ultrapure water and then mixed with 0.525 g (2.5 mmol) of H_3BTC dissolved in 15 ml of Ethanol. The mixture was stirred for 30 min, then, transferred to a Teflon autoclave liner and sealed to heat at 120 °C for 12 h. The obtained blue powder was washed several times with

ultrapure water and Ethanol and then dried at 25 °C [19].

Synthesis of Fe_3O_4 nanoparticles. Fe_3O_4 nanoparticles were synthesized by the co-precipitation method. First, 0.046 M of $FeCl_3.6H_2O$ and 0.023 M of $FeSO_4.7H_2O$ were dissolved in 100 ml of ultrapure water, and the solution was mixed at 80 °C. Then, 20 ml of 20% ammonium hydroxide (NH_4OH) was added to the aforementioned solution until it reached pH 11. After 45 min, the black precipitates of Fe_3O_4 nanoparticles in the solution were collected by magnetic separation. The separated Fe_3O_4 nanoparticles were washed three times with ultrapure water and once with Ethanol. The washed Fe_3O_4 nanoparticles were dried at 80 °C [20].

Hydrothermal Synthesis of Fe_3O_4 @HKUST-1. Fe_3O_4@HKUST-1 crystals were prepared by the following hydrothermal reaction: first, 1.087 g (4.5 mmol) of $Cu(NO_3)_2.3H_2O$ was dissolved in 15 ml of ultrapure water. Second, 0.525 g (2.5 mmol) of H_3BTC dissolved in 15 ml of Ethanol. Then, both solutions were mixed. The mixture was stirred for 30 min. Afterwards, 0.07 g of Fe_3O_4 was added to the mixture which was then transferred to a teflon autoclave liner and sealed to heat at 120 °C for 12 h. The obtained dark blue powder was washed several times with ultrapure water and Ethanol, then it was dried at 25 °C [19]. The dark blue powder produced in this synthesis was separated with external magnetic at 30 s.

Synthesis of HKUST-1@PVA. The preparation process of HKUST-1@PVA was as follows: PVA solution (4.0%, w/v) was obtained by dissolving PVA powder in DMSO/H_2O (4:1, V/V) mixture solvent at 90 °C with constant stirring till the solution was homogeneous. Then, HKUST-1 aqueous suspension was totally poured into the PVA solution. Continuously heating and stirring were operated till the volume of the solution was concentrated to the amount of the original PVA solution. A final concentration of 60 mg ml^{-1} (6.0%, w/v) was obtained. Next, the HKUST-1@PVA mixture was cooled to room temperature and was subjected to bath ultrasonication for 5 min for bubble removal. Then, HKUST-1@PVA was washed several times in ultrapure water to remove DMSO before using [7].

Adsorption Process

The effective parameters on the adsorption and removal efficiency, such as initial solution pH, amount of sorbent, and contact time were investigated and optimized. Different solutions were prepared by dissolving appropriate amounts of MLX in the range of 2-40 mg l^{-1} of distilled water and the calibration curve was obtained by measuring the absorbance at 361 nm. The adsorption process was carried out by adding a suitable amount (mg) of MOFs to 5 ml of MLX solutions. The solutions including the sorbent were mixed well with a magnetic stirrer for a suitable time (min). Subsequently, the solutions were separated; HKUST-1 and HKUST-1@PVA by centrifuge (10000 rpm) for 5 min, and Fe_3O_4@HKUST-1 by external magnetic field at 30 s. The remaining MLX concentrations were calculated by measuring the absorbance and using the calibration equations. The adsorption efficiency was quantified by the following equations:

$$q_e = \frac{(C_0 - C_e)V}{m_{ads.}} \quad (1)$$

$$q_t = \frac{(C_0 - C_t)V}{m_{ads}} \quad (2)$$

where, q_e and q_t (mg g^{-1}) are the amounts of the adsorbed MLX at equilibrium and any time, respectively. C_0 is the initial concentration of MLX, while C_e and C_t are the equilibrium concentration of MLX (mg l^{-1}) at any time. V (l) is the volume of the aqueous solution, and m_{ads} (g) is the MOFs weight. The adsorption isotherms were investigated by Eq. (1) and kinetic was studied by Eq. (2). For investigation of the efficiency of the adsorption process, the removal percentage of MLX was calculated by the following equation:

$$\%Removal = \frac{(C_0 - C_e)}{C_0} \times 100 \quad (3)$$

The equilibrium concentrations of MLX were calculated from the calibration equation resulting in the calibration plot (Fig. 1)

RESULTS AND DISCUSSION

Characterization

Various kinds of HKUST-1 were prepared regarding the aforementioned procedures. The MOFs were characterized by FT-IR, SEM, and VSM.

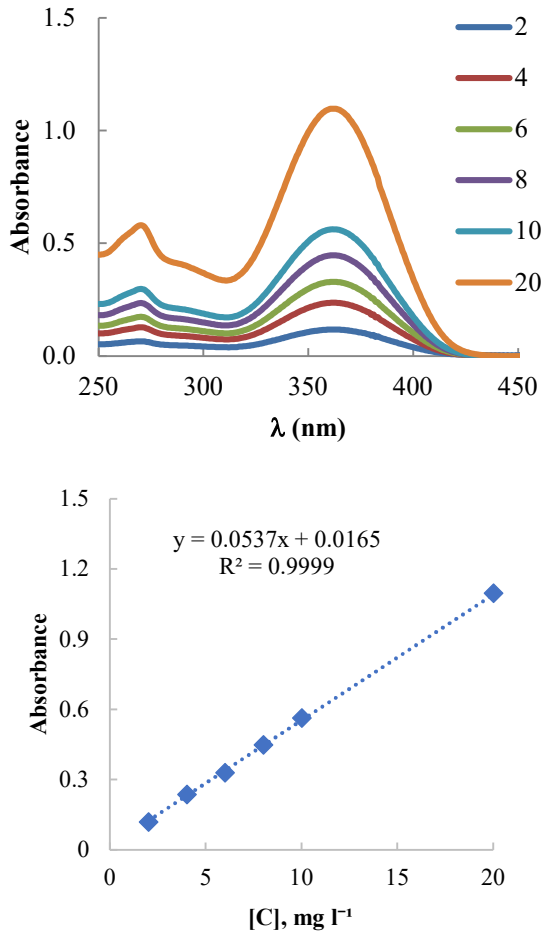

Fig. 1. Absorbance spectrum of MLX at different concentrations of 2-40 mg l^{-1} (a), a calibration curve of MLX at pH 7 (b).

Fourier Transform Infrared Spectroscopy (FT-IR)

In the FT-IR spectra of the various kinds of HKUST-1 (Fig. 2A: a, b, and c), the bands in the 1700-1500 and 1500-1300 cm^{-1} ranges were possibly related to -O-C-O- groups, while the ones at 1374 and 1559 cm^{-1} could indicate C=C stretching, demonstrating the incorporation of BTC in the framework. The wide band attributed to O-H stretching modes that appeared in the region of 3550-3200 cm^{-1} could be ascribed to the –OH of the crystalline water molecules within the HKUST-1 MOFs and O-H bands of PVA in HKUST-1@PVA. IR bands around 700 cm^{-1} are because of υ (C-H). The band at 680 cm^{-1} indicated bonding between Cu-O, while the band at 580, 790, and 890 cm^{-1} corresponded to the Fe-O groups of Fe_3O_4 in Fe_3O_4@HKUST-1 (Fig. 2A b).

Field Emission Scanning Electron Microscopy (FE-SEM)

The morphology of the MOFs was studied by field emission scanning electron microscopy (FE-SEM). Regarding Fig. 2B, (a) showed hydrothermal synthesized HKUST-1 with octahedral crystal structure, and (b) showed hydrothermal synthesized Fe_3O_4@HKUST-1 with octahedral crystal structure. In this synthesis method, the octahedral crystal structure of HKUST-1 remained intact in Fe_3O_4@HKUST-1. Furthermore, the octahedral crystal structure of HKUST-1@PVA was covered with PVA polymer (Fig. 2B (c)).

Vibrating Sample Magnetometry (VSM)

In order to study the magnetic behavior of Fe_3O_4 nanoparticles coupling with HKUST-1, magnetization measurements were recorded with VSM (Fig. 2C). The specific saturation magnetization value was measured to be 8.89 emu g^{-1} for Fe_3O_4 nanoparticles. The negligible coercivity Hc of hysteresis loop ($4O_e$) and consequently no remanence Mr (0.1 emu g^{-1}) indicated the superparamagnetic nature of the Fe_3O_4 nanoparticles [21].

Optimization of Experimental Conditions for the Removal of MLX

The effect of adsorption conditions was investigated and optimized to obtain more effective adsorption of MLX. The parameters include initial solution pH, amount of sorbent, and contact time between adsorbate and sorbent. A stock standard solution of MLX (100 mg l^{-1}) was prepared by dissolving the appropriate amount of meloxicam in 0.5 ml of 0.1 M NaOH and diluting the solution to 10 ml with distilled water. The daily used working solutions were prepared by diluting the stock solution to different concentrations.

Effect of the Initial Solution pH

Initial pH is a highly important parameter due to its strong effect on adsorption capacity. pH was adjusted by 0.1 M of HCl and NaOH solution. The effect of pH was studied between 5 and 10.5 with the initial concentration of MLX at 20 mg l^{-1} (Fig. 2). Generally, the adsorption recovery of MLX

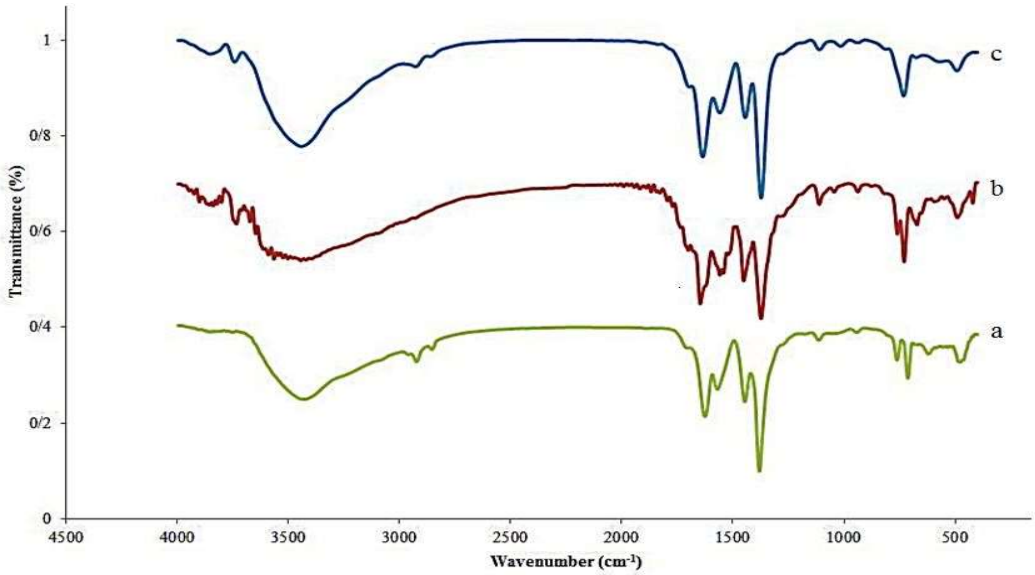

(A)

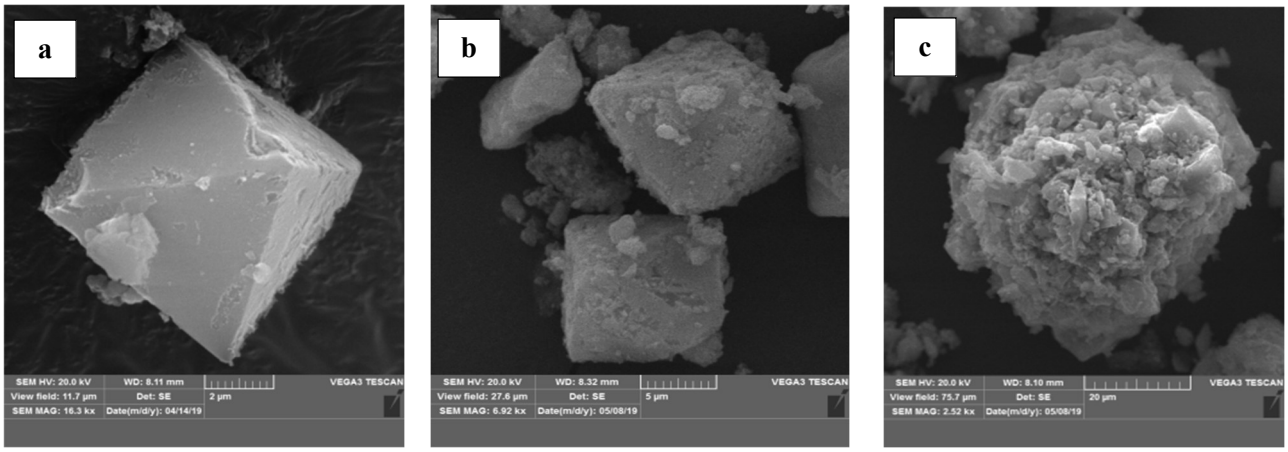

(B)

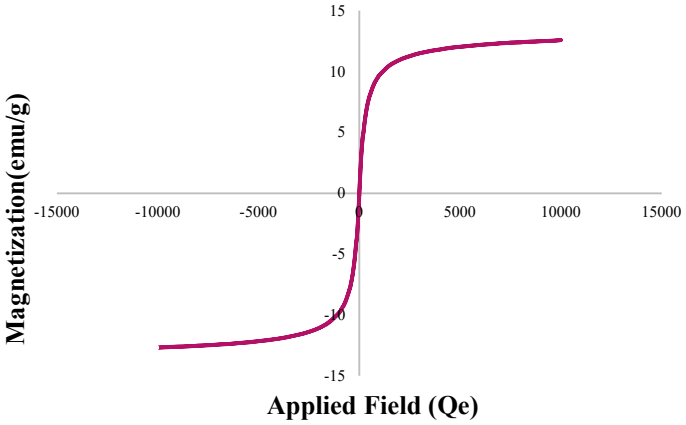

(C)

Fig. 2. (A): The FT-IR spectra of HKUST-1 (a), Fe_3O_4@HKUST-1 (b) and HKUST-1@PVA (c), (B): SEM of HKUST-1 (a), Fe_3O_4@HKUST-1 (b) and HKUST-1@PVA (c).

in 5, 7, and 9 was almost the same and by increasing pHs more than 9, removal decreases. The decrease in adsorption recovery in the alkaline pH (>9) is probably related to the effect of significant electrostatic interaction in the removal process. In industrial processes, the pH of wastewater varies widely, however, the adsorption mechanism was predominant at the neutral pH [17]. Since using these types of MOFs in wastewater treatment can be efficient, the pH = 7 was selected for further studies (Fig. 3a).

Effect of the Amount of Sorbent

One of the effective parameters of the adsorption capacity is the amount of sorbent. This factor was tested to obtain the best removal percentage by adding 0.3-1.0 mg of the sorbents to 5 ml of MLX (20 mg l^{-1}) solution. The best removal percentage of MLX was obtained at the amounts of 0.7 mg for HKUST-1, 0.7 mg for Fe_3O_4@HKUST-1, and 0.5 mg for HKUST-1@PVA and selected for further experiments (Fig. 3b).

Effect of Contact Time

The key point in the adsorption process is the equilibrium time which is the required time for the interaction between adsorbate and sorbent. Hence, the effect of contact time on the removal of MLX was studied from 0.5 min to 10 min for the three types of HKUST-1. Each time, the removal percentage was calculated based on Eq. (3). The best results were obtained in 5, 5, and 3 min for HKUST-1, HKUST-1@PVA, and Fe_3O_4@HKUST-1, respectively (Fig. 3c).

Adsorption Isotherms

The equilibrium relationship between the sorbent and MLX was described by adsorption isotherms under different initial MLX concentrations at pH 7.0. The adsorption isotherms of MLX onto HKUST-1, Fe_3O_4@HKUST-1, and HKUST-1@PVA were plotted based on Freundlich and Langmuir models.

Freundlich model: The Freundlich equation is mentioned below:

$$logq_e = logK_F + \frac{1}{n}logC_e \quad (4)$$

where q_e is the equilibrium adsorption capacity (mg g^{-1}), C_e

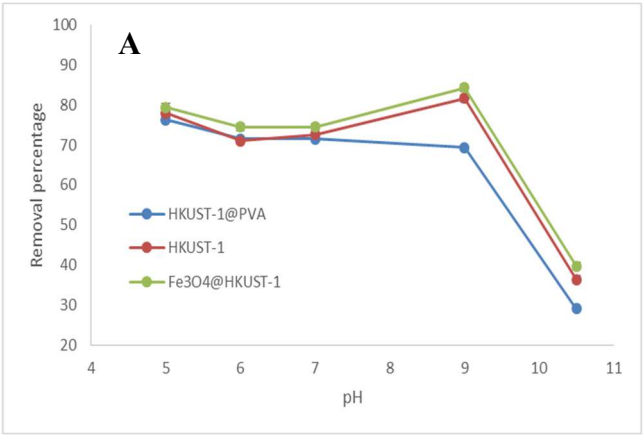

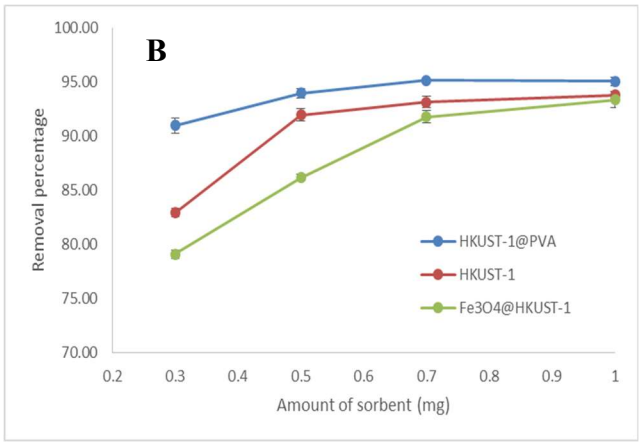

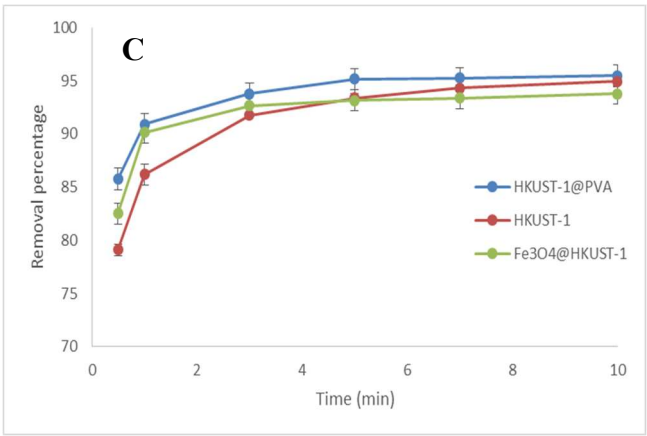

Fig. 3. (A): Effect of pH (5, 6, 7, 9, 10.5) on removal percentage of 20 mg l^{-1} of MLX in the presence of three MOFs (n = 3), (B): Effect of amount of sorbent (0.3, 0.5, 0.7, 1 mg) on removal percentage of 20 mg l^{-1} of MLX in the presence of three MOFs (n = 3), (C): Effect of Time (0.5, 1, 3, 5, 7, 10 min) on removal percentage of 20 mg l^{-1} of MLX in the presence of three MOFs (n = 3).

is the equilibrium concentration of MLX (mg l^{-1}), K_F and n are Freundlich constants. The parameters of the Freundlich isotherm model are summarized in Table 1 and the curve fitting results are depicted in Fig. 4.

The Freundlich model for all three MOFs fits to describe the process of adsorption based on the correlation coefficient

Table 1. Freundlich Isotherm Parameters of MLX Adsorption onto HKUST-1, Fe_3O_4@HKUST-1, and HKUST-1@PVA at Curve $\ln q_e$ *vs*. $\ln C_e$

MOF	Freundlich		
	K_F (mg g^{-1} (l $mg^{-1})^{1/n}$)	n	R^2
HKUST-1	3.02E+03	0.74	0.9914
Fe_3O_4@HKUST-1	7.24E+03	0.99	0.9948
HKUST-1@PVA	7.99E+04	1.49	0.9825

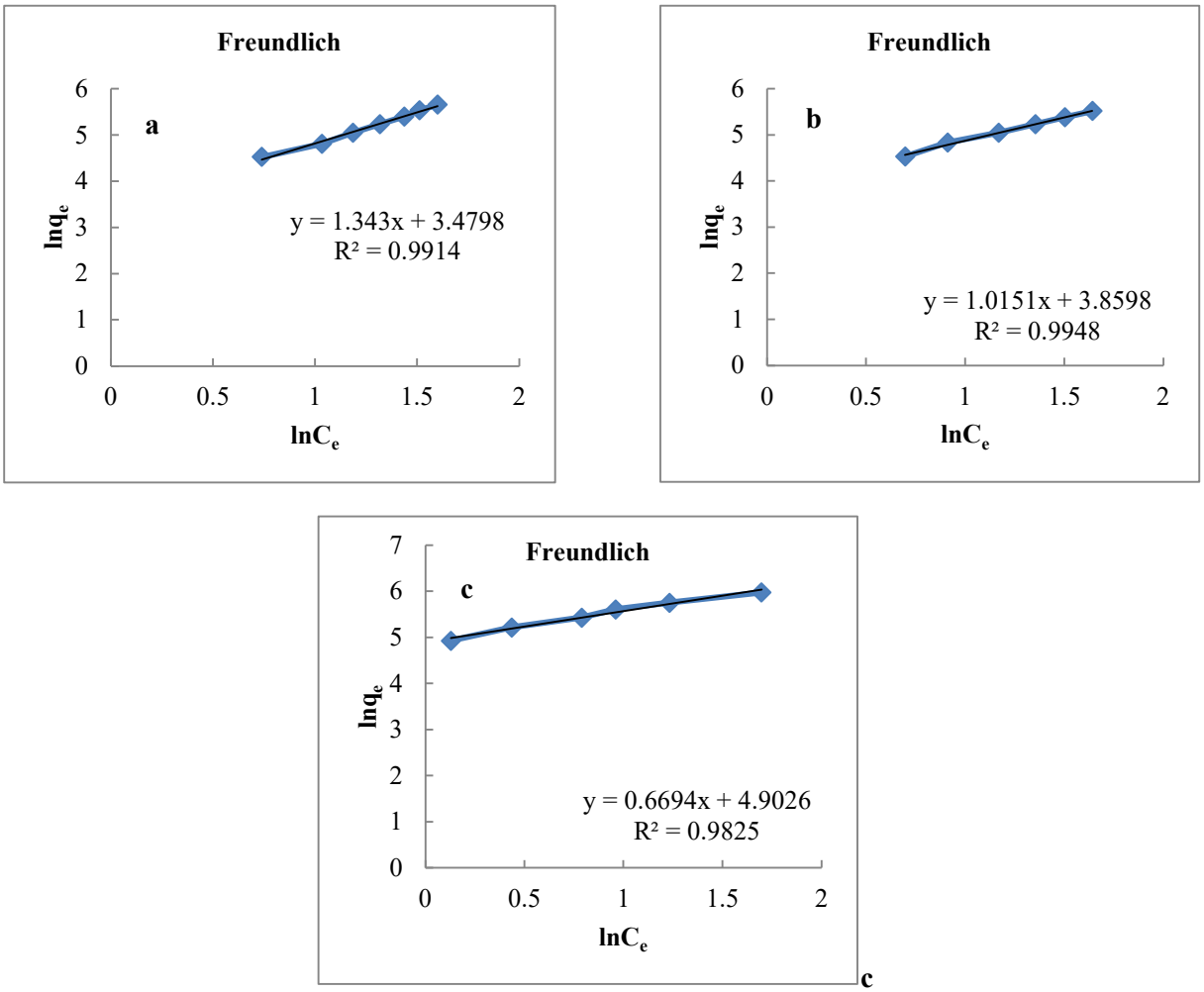

Fig. 4. Freundlich isotherm model curves of MLX onto HKUST-1 (a), Fe_3O_4@HKUST-1 (b), and PVA@HKUST-1 (c).

(R^2) values (nearly 1). Thus, the adsorption of MLX onto these MOFs can be attributed to the chemical interactions of π-π and/or hydrogen bonding. In addition, n < 1 at the Freundlich model for HKUST-1 and Fe_3O_4@HKUST-1 indicated the chemical adsorption of MLX onto the adsorbents. Further, n > 1 at the Freundlich model for HKUST-1@PVA indicated the physical adsorption of MLX onto the desired sorbent [22].

Langmuir model: The Langmuir equations are mentioned below:

$$\frac{1}{q_e} = \frac{1}{K_{ML}C_e q_{max}} + \frac{1}{q_{max}} \quad (5)$$

Langmuir model for Fe_3O_4@HKUST-1 (Table 2, and Fig. 5c) and HKUST-1@PVA (Table 2, and Fig. 5d) was fitted to describe this adsorption process. Thus, the adsorption of MLX onto these MOFs can be considered to be monolayer adsorption (in HKUST-1@PVA and Fe_3O_4@HKUST-1) [22]. The values of q_{max} were obtained as 883.33, and 2.50E+03 mg g^{-1} for HKUST-1@PVA and Fe_3O_4@HKUST-1), respectively.

The experiment data of Langmuir adsorption parameters for HKUST-1 (q_{max} and K_{ML}) has negative intercepts, (Table 2 and Fig. 5a) that may be due to system cumulative errors of the volumetric method, and errors of adsorbed phase in free space volume [22] or low concentration of analyte and high quantity of sorbent [23] and suggesting its adsorption behavior does not follow the assumption of the Langmuir approach [24] and it can be solved by nonlinear model. So, In this case, a nonlinear Langmuir isotherm (Table 2 and Fig. 5b) was studied based on the reference [25] to solve the problem. The nonlinear Langmuir equation is mentioned below; the plot is q_e *vs*. C_e [25].

$$q_e = \frac{q_{max}K_{ML}C_e}{1+K_{ML}C_e} \quad (6)$$

The calculated values of q_e were -384.62 and 7.08E + 05 mg g^{-1} for HKUST-1 at normal and nonlinear Langmuir isotherm.

Adsorption Kinetics

The adsorption rate is an important characteristic of a given adsorbent. To evaluate the adsorption rate of

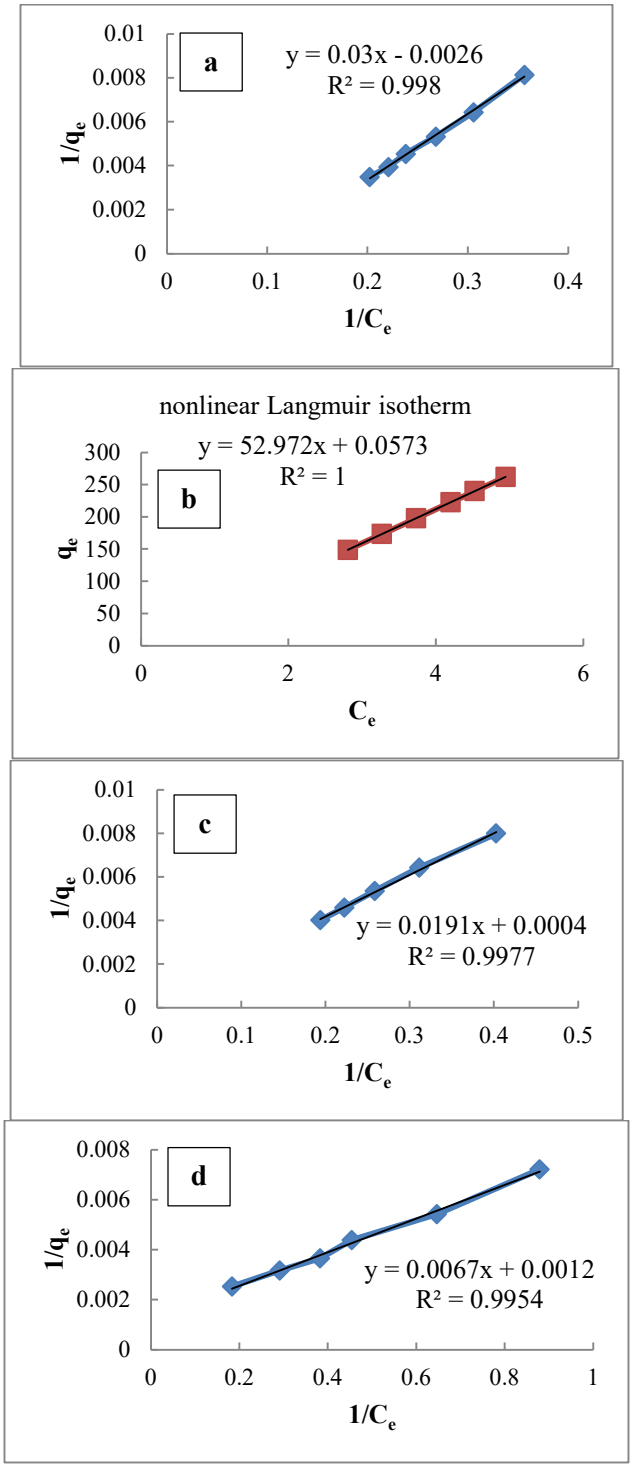

Fig. 5. (a) Langmuir Isotherm model curves of MLX onto HKUST-1, ($1/q_e$ *vs*. $1/C_e$), (b) Nonlinear Langmuir isotherm model curve of MLX onto HKUST-1, (c) Langmuir Isotherm model curves of MLX onto Fe_3O_4@HKUST-1, ($1/q_e$ *vs*. $1/C_e$), (d) Langmuir Isotherm model curves of MLX onto HKUST-1@PVA, ($1/q_e$ *vs*. $1/C_e$).

Table 2. Langmuir Isotherm Model Results of MLX onto HKUST-1, Fe_3O_4@HKUST-1, and HKUST-1@PVA

Isotherm model:	Normal Langmuir isotherm Curve ($1/q_e$ *vs.* $1/C_e$)			Modified Langmuir isotherm Curve ($1/q_e$ *vs.* $1/C_e$)			*Nonlinear analysis* Curve (q_e *vs.* C_e)		
Equation:	$\frac{1}{q_e}=\frac{1}{K_{ML}C_e q_{max}}+\frac{1}{q_{max}}$			$\frac{1}{q_e}=\frac{C_s}{K_{ML}q_{max}C_e}+\frac{(K_{ML}-1)}{K_{ML}q_{max}}$			$q_e=\frac{q_{max}K_{ML}C_e}{1+K_{ML}C_e}$		
MOF \ Factor	q_{max}	K_{ML}	R^2	q_{max}	K_{ML}	R^2	q_{max}	K_{ML}	R^2
HKUST-1	-384.62	-0.09	0.998	-778.69	-0.98	0.998	7.08E+05	7.49E-05	1
Fe_3O_4@HKUST-1	2.50E+03	0.02	0.9977	807.94	1.48	0.9977			
HKUST-1@PVA	833.33	0.18	0.9954	669.41	5.08	0.9954			

Table 3. Kinetic Model Parameters of MLX Adsorption onto HKUST-1, Fe_3O_4@HKUST-1, and HKUST-1@PVA

MOF	MLX C_0 (mg l^{-1})	q_e (mg g^{-1})	pseudo-first-order model k_1 (min^{-1})	$q_{e,cal}$ (mg g^{-1})	R^2	pseudo-second-order model K_2 (g mg^{-1} min^{-1})	$q_{e,cal}$ (mg g^{-1})	R^2
HKUST-1	20	122.81	7.98E-02	1.90E+01	0.9848	1.23E-04	1.00E+03	1
Fe_3O_4@HKUST-1	20	125.11	3.66E-02	9.77E+00	0.5034	1.10E-05	3.33E+03	1
HKUST-1@PVA	20	184.53	2.67E-02	2.50E+01	0.4837	4.46E-05	2.00E+03	0.9998

HKUST-1, Fe_3O_4@HKUST-1, and HKUST-1@PVA, the effect of the contact time on MLX adsorption (*i.e.* adsorption kinetics) was examined at initial concentrations of MLX (20 mg l^{-1}) at optimum conditions for each of them. The pseudo-first-order (Eq. (7)) and pseudo-second-order (Eq. (8)) kinetic models are given in the following equations:

$$log(q_e - q_t) = log q_e - \frac{k_1 t}{2.303} \quad (7)$$

$$\frac{t}{q_t} = \frac{1}{k_2 q_e^2} + \frac{1}{q_e} \quad (8)$$

q_t (mg g^{-1}) and q_e (mg g^{-1}) are the amounts of adsorbed MLX at time t (min) and the amount at adsorption equilibrium, respectively, and k_1 (min^{-1}) and k_2 (g mg^{-1} min^{-1}) are the pseudo-first-order and pseudo-second-order rate constants, respectively.

The fitting results (Table 6) show that the adsorption of MLX onto all three sorbents could be well described by the pseudo-second-order kinetic model ($R^2 > 0.99$) better than the pseudo-first-order model. The values of k_2 were obtained as 1.23E-04, 1.10E-05 and 4.46E-05 g mg^{-1} min^{-1} for HKUST-1, Fe_3O_4@HKUST-1, and HKUST-1@PVA, respectively.

Thermodynamic Study

The adsorption thermodynamic was studied at different temperatures. The change of standard free energy (G_0), standard enthalpy (H_0), and standard entropy (S_0) were calculated by the following equations:

$$\Delta G^0 = \Delta H^0 - T\Delta S^0 \quad (9)$$

$$ln\frac{q_e}{C_e} = \frac{\Delta S^0}{R} - \frac{\Delta H^0}{RT} \quad (10)$$

K_0 (q_e/c_e) is the thermodynamic equilibrium constant, C_s is the amount of MLX adsorbed per mass of MOFs (mg g^{-1}), C_e is the equilibrium concentration (mg l^{-1}), T is the temperature in Kelvin, and R (8.314 J mol^{-1} K) is the ideal gas constant (Table 4). The negative values of change in Gibbs free energy (ΔG°) at different temperatures demonstrate the spontaneous

Table 4. Thermodynamic Parameters of MLX Adsorption onto HKUST-1, Fe_3O_4@HKUST-1, and HKUST-1@PVA

MOF	T (K)	ΔG (kJ mol^{-1})	ΔS (kJ mol^{-1} K^{-1})	ΔH (kJ mol^{-1})
HKUST-1	298	-1.10E+04	5.80E+01	6.33E+03
	303	-1.13E+04		
	313	-1.18E+04		
	323	-1.24E+04		
Fe_3O_4@HKUST-1	283	-7.13E+03	1.36E+02	3.15E+04
	293	-8.49E+03		
	303	-9.86E+03		
	313	-1.12E+04		
HKUST-1@PVA	283	-1.04E+04	1.01E+02	1.80E+04
	293	-1.15E+04		
	298	-1.20E+04		
	303	-1.25E+04		

nature of MLX adsorption onto the MOFs. More negative value at higher temperatures reveals that the adsorption was more spontaneous with the increase in temperature. The positive ΔH° value demonstrates that the adsorption of MLX onto MOFs is endothermic. Similarly, the increase in entropy must overcome the deficiency of the endothermic process so that TΔS > ΔH. Since the effect of temperature is to "magnify" the influence of a positive ΔS, the process will be spontaneous at temperatures above T = ΔH/ΔS.

Reusability

Desorption and regeneration experiments were conducted in order to investigate the reusability of the three types of HKUST-1. In a typical adsorption-desorption cycle, a certain amount of each MOF was dispersed in a solution containing 20 mg l^{-1} of MLX, followed by stirring for different equal times. After adsorption equilibrium, the adsorbent was separated and the amount of the adsorbed MLX was determined. The used adsorbent was then regenerated by mixing with 5 ml of methanol and/or acetonitrile solvents under ultrasonic irradiation for certain minutes. The amount of desorbed MLX was subsequently determined. Then, the adsorbent was used in the next adsorption-desorption cycle. The reusability of HKUST-1 was tested at 5 min in 5 ml of methanol and 5 ml of acetonitrile (Fig. 6a and b, respectively). The results showed over 90% reusability. No obvious reduction was seen in the adsorption capacity while increasing the recycle times. After five cycles, the adsorption capacity decreased to <7% in methanol and <3% in acetonitrile, which is possibly due to the higher MLX solubility in acetonitrile than in methanol.

HKUST-1@PVA was tested at 3 min in 5 ml of methanol and showed over 90% reusability (Fig. 6c). No obvious reduction was seen in the adsorption capacity while increasing the recycle times and after seven cycles, the adsorption capacity decreased to <5% in methanol. Functionalization of HKUST-1 with polyvinyl alcohol increased the adsorption capacity of the MOF. Thus the aforementioned step helped HKUST-1@PVA regenerate more than HKUST-1 regeneration in methanol.

Fe_3O_4@HKUST-1 was tested at 1 min in 5 ml of acetonitrile and showed over 90% reusability (Fig. 6d). No obvious reduction was seen in the adsorption capacity while increasing the recycle times and after six cycles, the adsorption capacity decreased to <5% in acetonitrile. Functionalization of HKUST-1 with Fe_3O_4 increased the adsorption capacity of the MOF. Thus the aforementioned step helped Fe_3O_4@HKUST-1 regenerate as much as HKUST-1 regenerated in acetonitrile.

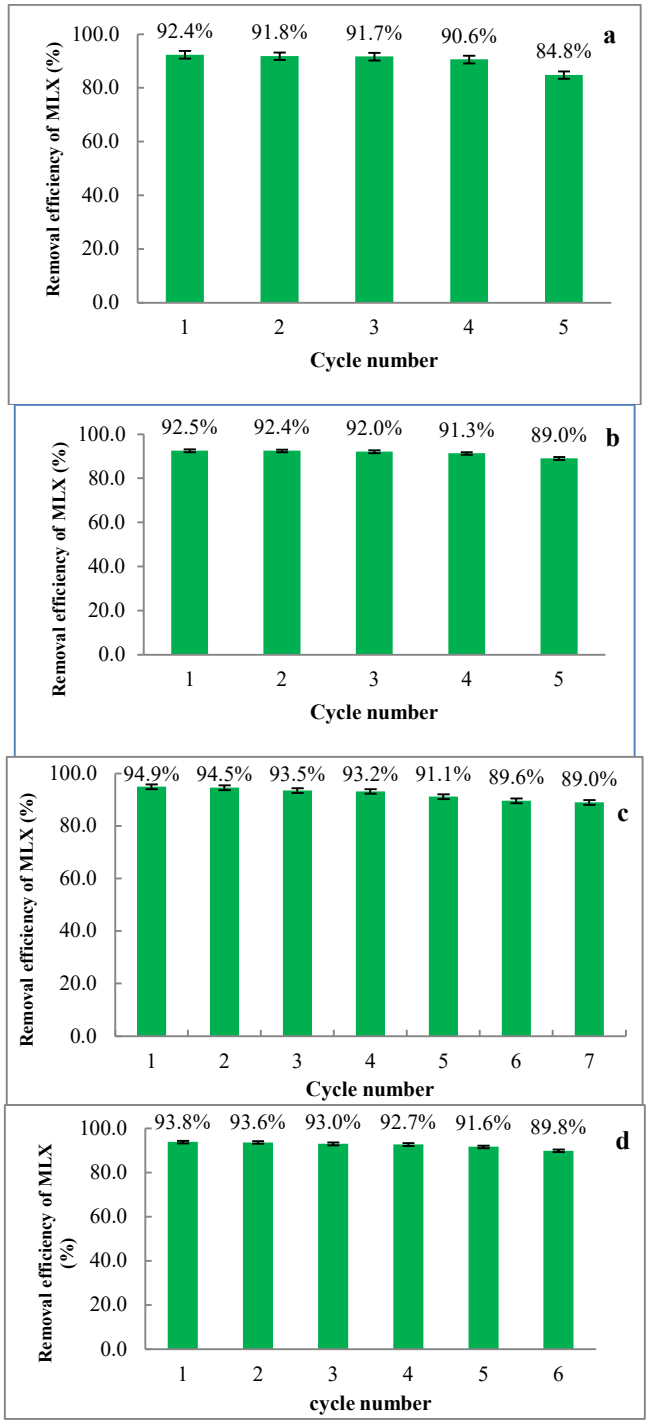

Fig. 6. (a) Reusability of HKUST-1 with methanol (5 ml) for 5 min and 25 °C, (b) Reusability of HKUST-1 with acetonitrile (5 ml) for 5 min and 25 °C, (c) Reusability of HKUST-1@PVA with methanol (5 ml) for 3 min and 25 °C, (d) Reusability of Fe_3O_4@HKUST-1 with acetonitrile (5 ml) for 1 min and 25 °C.

Usability in Different Volumes of Initial Solution

HKUST-1, HKUST-1@PVA and Fe_3O_4@HKUST-1 were tested in 2, 5, 10, 20, and 40 ml of the initial solution of MLX to investigate the effect of volume on removal percentage and adsorption capacity. Results indicated that the removal ability is amazingly over 70% with 40 ml of the initial solution of MLX (Figs. 7A, B, and C parts (a)). In addition, increasing adsorption capacity was detected with increasing the volume of the initial solution (Figs. 7A, B, and C parts (b)).

Adsorption Mechanism

The possible interactions between HKUST-1 and MLX are supposed as mentioned below regarding the porous structure of the proposed HKUST-1s and the structure features of MLX. MLX is trapped in the pores of the proposed HKUST-1s; the coordination bonds interaction could be formed between the active sites of Cu in the proposed HKUST-1s and the phenolic oxygen atoms in MLX; hydrogen bonds interaction between carboxyl in the proposed HKUST-1s and secondary amine in MLX and also π-π interactions occur between phenyl rings of the proposed HKUST-1s and MLX; Van der Waals interactions take place; Ion-π interactions happen between $C\text{-}O^-$ and C=X (X= C, O, N or S), and hydrophobic interaction could be occurred.

The phenolic and amine groups in the chemical structure of meloxicam cause its polarity, while the aromatic, SO_2, and methyl groups are nonpolar [26]. MLX polarity is suggested to be another cause for trapping MLX into the polar pores of HKUST-1s. However, polar surface area (99.6 $Å^2$), polarizability, the number of hydrogen acceptors (5), and hydrogen donors (2) (www.drugbank.ca) are suggested to be other causes for trapping MLX into the polar/apolar pores of the proposed HKUST-1s resulting in a high removal percentage of MLX from aqueous solution. Due to their π-electrons, the apolar adsorbents have favorable interactions with the copper sites in the framework [12].

Comparison of the Proposed MOFs with other Materials

A comparison of the present method with other approaches for removing MLX by different materials is shown in Table 5, considering the least amount of sorbents at

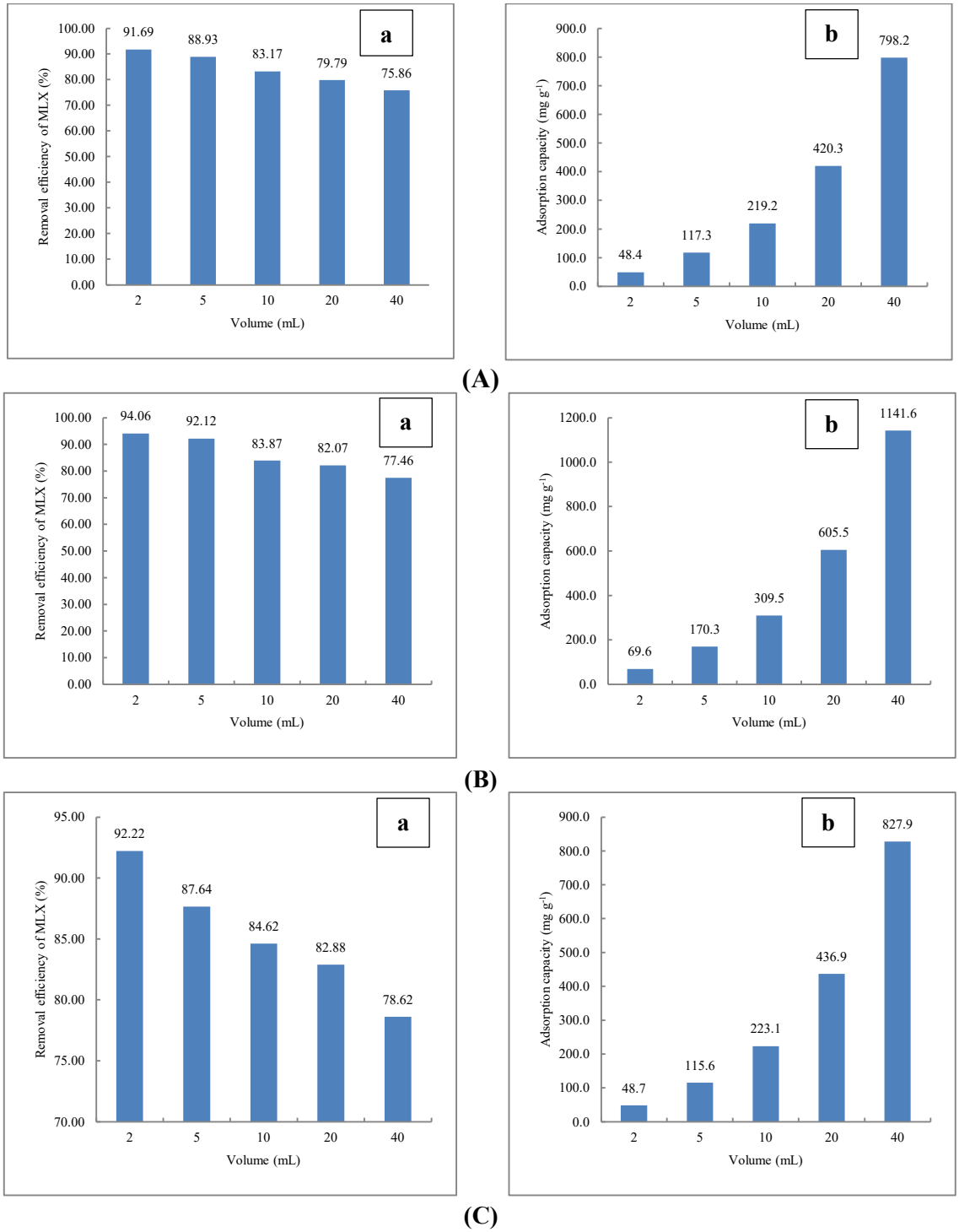

Fig. 7. (A): Usability of HKUST-1 in different volumes of the initial solution of MLX (2, 5, 10, 20, and 40 ml) (a), and adsorption capacity (b), (B): Usability of HKUST-1@PVA in different volumes of the initial solution of MLX (2, 5, 10, 20 and 40 ml) (a), and adsorption capacity (b), (C): Usability of Fe_3O_4@HKUST-1 in different volumes of initial solution of MLX (2, 5, 10, 20 and 40 ml) (a), and adsorption capacity (b).

Table 5. Comparison of the Proposed MOFs with Previously Reported Materials for the Removal of Meloxicam

Sorbent	Removal percentage	Equilibrium time	The amount of sorbent (mg)	Initial solution volume (ml): concentration (mg l^{-1})	Reusability (removal efficiency: cycles)	Method	Adsorption capacity (mg g^{-1})	Ref.
HKUST-1	93.36	5 min	0.7	5:20	above 90%:4	UV-Vis[d]	122.81	Present study
Fe_3O_4@HKUST-1	93.14	3 min	0.7	5:20	above ~90%:6	UV-Vis[d]	125.11	Present study
HKUST-1@PVA	95.16	5 min	0.5	5:20	above ~90%:7	UV-Vis[d]	184.53	Present study
Fe_3O_4/SiO_2/GMA-S-SH	55 ± 2	4 h	25	2:0.6	NR[7]	UV-Vis[d]	NR[7]	[27]
	88 ± 2	48 h	25	2:0.6	above 80%:4	UV-Vis[d]	NR[7]	[27]
Fe_3O_4/SiO_2/GMA-S-SH/laccase	60 ± 2	4 h	25	2:0.6	NR[7]	UV-Vis[d]	NR[7]	[27]
	92	48 h	25	2:0.6	above 80%:4	UV-Vis[d]	NR[7]	[27]
Fe_3O_4@MIL-100(Fe)	NR[7]	2 h	40	50:20	above 95%:5	MSPE-UV[e]	123.1	[28]
PAni-CF[a]	NR[g]	4 min	17.5	3.5:0.1	NR[7]	HPLC-DAD[f]	169.6	[29]
PAni[b]	NR[g]	6 min	17.5	3.5:0.1	NR[g]	HPLC-DAD[f]	86.22	[29]
CF[c]	NR[g]	2 min	17.5	3.5:0.1	NR[g]	HPLC-DAD[f]	160.8	[29]

[a]Polyaniline-deposited cellulose fiber composite (PAni-CF), [b]Polyaniline (PAni), [c]Cellulose fiber (CF), [d]Ultraviolet-visible spectrophotometry (UV-Vis), [e]Magnetic solid phase extraction-Ultraviolet-visible spectrophotometry (MSPE-UV), [f]Liquid chromatograph coupled with a diode array detector (HPLC-DAD), [g]Not Reported (NR).

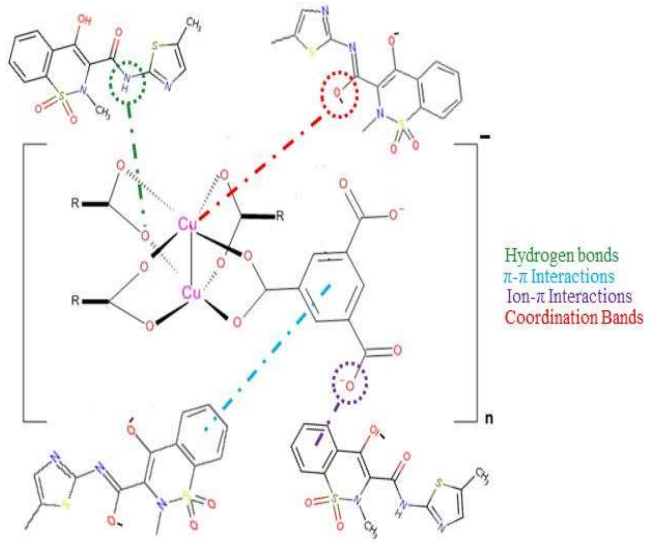

Scheme 1. Possible adsorption mechanism of MLX on HKUST-1

short equilibrium times, the adsorbing ability of the proposed MOFs is much stronger than that of other materials in addition excellent removal percentage and adsorption capacity, and good reusability with high removal efficiency (%).

CONCLUSIONS

In the present research, three types of HKUST-1 were synthesized; the removal applicability was studied by UV-Vis spectrophotometry. The MLX removal from aqueous solution was investigated regarding the adsorption isotherms, kinetic, and thermodynamics of the sorbent. The adsorption process was spontaneous and endothermic based on the determined thermodynamic parameters (free energy, enthalpy, and entropy). Magnetization was used to increase

the speed of separation of MOF particles from water by an external magnetic field and showed almost similar results in performance with HKUST-1.PVA was functionalized for enhancing the polarity of HKUST-1, resulting in an increased adsorption capacity for the polar analyte. The results confirm that the proposed MOFs are efficient and promising sorbents, and have potential applications for the removal of environmental pollutants such as drugs from water and wastewater during the treatment process. However, the performance of the sorbents is not good for selective separation of pollutants due to their surface OH groups. However, the application of porous adsorbents can be proposed as a suitable and cost-effective alternative for effective and efficient water treatment.

ACKNOWLEDGMENT

We gratefully acknowledge from financial support from the Research Council of Alzahra University.

REFERENCES

[1] E.Y. Tahmasebi, M. Masoomi, Y. Yamini, A. Morsali, RSC Adv. 6 (2016) 40211.

[2] S.H. Huo, H.Y. An, J. Yu, X.F. Mao, Z. Zhang, L. Bai, Y.F. Huang, P.X. Zhou, J. Chromatogr. A 1517 (2017) 18.

[3] Y. Bian, N. Xiong, G. Zhu, Processes 6 (2018) 122.

[4] R. De. Andrade, M.F. Oliveira, M.G.C. Silva, M.G.A. Vieira, Ind. Eng. Chem. Res. 57 (2018) 3103.

[5] X. Shi, X. Chen, Y. Hao, L. Li, H. Xu, M. Wang, J. Chromatogr. B Analyt Technol. Biomed. Life Sci. 1086 (2018) 146.

[6] K. Chullasat, P. Nurerk, P. Kanatharana, Anal. Chim. Acta 961 (2017) 59.

[7] Y. Wang , Y. Zhang, J. Cui, S. Li, M. Yuan, T. Wang, Q. Hu, X. Hou, Anal. Chim. Acta 1022 (2018) 45.

[8] S. Loera-Serna, M.A. Oliver-Tolentino, M.d.L. López-Núñez, A. Santana-Cruz, A. Guzmán-Vargas, R. Cabrera-Sierra, H.I. Beltrán, J. Flores, J. Alloys Compd. 540 (2012) 113.

[9] M. Mohammadnejad, A. Moeinipour, Int. J. Ion Mob. Spect. 23 (2020) 105.

[10] T.R.C. Van Assche, T. Duerinck, J.J. Gutierrez-Sevillano, S. Calero, G.V. Baron, J.F.M. Denayer, J. Phys. Chem. C 117 (2013) 18100.

[11] M. Mohammadnejad, M. Fakhrefatemi, J. Mol. Struct. 1224 (2021) 129041.

[12] S. Liu, S. Li, W. Yang, F. Gu, H. Xu, T. Wang, D. Sun, X. Hou, Talanta 194 (2018) 514.

[13] Mohammadnejhad, M. Moeinipour, A. Nanoscale, 8 (2021) 22.

[14] N. Seedher, S. Bhatia, AAPS Pharm. Sci. Tech. 4 (2003) 36.

[15] L. Zhao, N. Liang, X. Lun, X. Chen, X. Hou, Anal. Methods 6 (2014) 6956.

[16] M. Petrovic, B. Skrbic, J. Zivancev, L. Ferrando-Climent, D. Barcelo, Sci. Total Environ. 468 (2014) 415.

[17] A.H. Nadim, M.A. Al-ghobashy, RSC Adv. 5 (2015) 104981.

[18] L. Li, X.L. Liu, M. Gao, W. Hong, G.Z. Liu, L. Fan, B. Hu, Q.H. Xia, L. Liu, G.W. Song, Z.S. Xu, J. Mater. Chem. A 2 (2014) 1795.

[19] R. Abhinayaa, G. Jeevitha, D. Mangalaraj, N. Ponpandian, K. Vidhya, J. Angayarkanni, Colloids Surf. B 169 (2018) 395.

[20] M. Mahdavi, F. Namvar, M. Bin Ahmad, R. Mohamad, Molecules 18 (2013) 5954.

[21] V. Tharaneedhar, P.S. Kumar, A. Saravanan, C. Ravikumar, V. Jaikumar, SUSMAT 11 (2016) 1.

[22] P. Yalkowsky, H. Samuel, Y.J. He, Aqueous solubility data, ISBN 9780367384173. CDC Press, 2010.

[23] S. Azizian, S. Eris, L.D. Wilson, Chem. Phys. 513 (2018) 99.

[24] J.S. Kiurski, S. Adamovic, J. Krstic, Glob. Nest J. 14 (2012) 18.

[25] N.B.M. Hamzaoui, B. Bestani, J. Mater. Environ. Sci. 9 (2018) 1110.

[26] S.K.A. Mudalip, M.R.A. Bakar, P. Jamal, F. Adam, J. Chem. Eng. Data 58 (2013) 3447.

[27] S.M. Siddeeg, A. Amari, M.A. Tahoon, N.S. Alsaiari, F.B. Rebah, Alex. Eng. J. 59 (2020) 905.

[28] S. Liu, Y. Zhao, T. Wang, N. Liang, X. Hou, J. Chem. Eng. Data. 64 (2019) 2997

[29] F.V.A. Dutra, B.C. Pires, T.A. Nasscimento, V. Mano, K. B. Borges, RSC Adv. 7 (2017) 12639.

[30] Y. Dai, Q. Tang, Z. Zhang, C. Yu, H. Li, L. Xu, Sh. Zhang, Z. Zou, RSC Adv. 8 (2018) 38681.